Journal of Polymer Research (2018) 25: 196
https://doi.org/10.1007/s10965-018-1586-3

ORIGINAL PAPER

Morphology and property changes in PLA/PHBV blends as function of blend composition

Gurmeet S. Kanda[1] · Ilham Al-Qaradawi[1] · Adriaan S. Luyt[2]

Received: 18 April 2018 / Accepted: 2 August 2018 / Published online: 14 August 2018

Abstract

PLA/PHBV blends were prepared by melt mixing. The morphology and physical properties of the blends and neat polymers were investigated. Scanning electron microscopy (SEM) studies provided evidence of interfacial cavities and weak interfacial interaction between the two polymers, and no obvious co-continuous morphology was observed in any of the investigated blends. Positron annihilation lifetime spectroscopy (PALS) indicated the presence of open-volume cavities with sub-nanometre diameters; far smaller than observed from the SEM images. The mean size and relative concentration of these cavities increased with increasing PHBV content. A weak negative deviation in the mean size for low PHBV content possibly indicates some degree of partial miscibility. The glass transition temperature of PLA in the blends decreased with increasing PHBV content, and offers support to some PHBV being miscible with the PLA. The degree of crystallinity in the blends show interesting behaviour that may be explained in terms of the complex morphology observed for these blends. The thermal conductivity of the samples varied with composition, but increased with increasing PHBV content, which was probably related to the increasing crystallinity. Both the tensile strength and Young's modulus decreased with increasing PHBV content for the sequence of blends, and both parameters exhibited maximum values for 10 wt.% PHBV. For samples between 50/50 and 10/90 PLA/PHBV the tensile strength and Young's modulus were comparable to or lower than those for both the neat polymers.

Keywords Poly(lactic acid) · Poly(3-hydroxybuterate-co-hydroxyvalerate) · Blends · Morphology · Characterization · Positron annihilation lifetime spectroscopy

Introduction

The use of polymers has become widespread due to the low manufacturing costs and broad range of applications industry [1–4]. However, the high volume of production, short service lifespan, and high durability of most polymers has resulted in an increase in environmental pollution [5]. Consequently, significant research has been conducted into plastics that not only can be produced from sustainable, non-petrochemical, sources (bioplastics) but also are biodegradable, for example, poly(lactic acid) (PLA) and poly(3-hydroxybutyrate-co-hydroxyvalerate) (PHBV).

PLA is a biodegradable bioplastic that can be produced from renewable sources, for example corn starch [6, 7]. It can be readily utilised by a number of manufacturing processes, e.g., injection moulding, thermoforming, and extrusion [8, 9]. Furthermore, it exhibits high strength and modulus properties [7]. However, it suffers from low thermal stability, is hydrophobic, and brittle [10–12]. PHBV is a polyhydroxyalkanoate type polymer with randomly distributed 3-hydoxybutyrate and 3-hydroxyvalerate groups. PHBV is a biodegradable biopolymer that can be synthesised by natural mechanisms [13]. It exhibits biocompatibility and, therefore, has numerous biomedical applications. [14]. However, it is a brittle material and exhibits low tensile strength and modulus characteristics [15–17].

A number of techniques have been developed to improve the properties of polymers, e.g., co-polymerisation and incorporation of fillers. Blending of two, or more, polymers in the production phase provides a simple and cost-effective method to produce a new material that can display improved physical and mechanical characteristics to either of the constituents. However, an improvement in one property may result in the deterioration of another [18, 19].

✉ Adriaan S. Luyt
aluyt@qu.edu.qa

[1] Department of Mathematics, Statistics and Physics, Qatar University, Doha, Qatar

[2] Center for Advanced Materials, Qatar University, Doha, Qatar

The mechanical properties of PLA-PHBV blends are often characterised using tensile testing and it is routinely reported that a decrease in tensile strength and Young's modulus is observed with increasing PHBV concentration [16, 20–22]. However, Zembouai and co-workers [23–25] characterised blends with 25, 50, and 75 wt.% of PHBV and observed an increase in Young's Modulus with PHBV content. Whilst, González-Ausejo et al. [26] reported that blends with high PHBV content (75 wt.%) exhibited higher tensile strength and Young's modulus values than pure PLA.

Differential scanning calorimetry (DSC) and dynamic mechanical analysis (DMA) measurements to obtain the glass transition temperatures (T_g) have been widely reported. Researchers have routinely observed two T_g values for PLA-PHBV blends, and that the T_g for PLA reduces with increasing PHBV content [16, 20, 23–29]. In contrast, research by Ma et al. and Liu et al. observed no distinct change in T_g for blends with PHBV contents between 0 and 50 wt.% and 5–30 wt.%, respectively [21, 22]. On the basis of these studies, researchers have concluded that these materials form an immiscible blend [16, 20–32].

The properties of polymers and their blends are closely related to their morphology or free volume, where the latter is defined as the unoccupied volume within a material. Positron annihilation lifetime spectroscopy (PALS) is a non-destructive spectroscopic characterisation method that is capable of detecting sub-nanometre diameter open-volumes with parts per million concentration levels. Positrons emitted from a radioactive source are implanted into the material of interest where they quickly thermalize and can annihilate with electrons in the material under study, where the time taken to annihilate depends upon the electron density of the material. In the case of polymers, the large open-volume regions can act as trapping sites and permit additional decay modes where the positron and electron are in a bound state known as a positronium.

The positronium bound state comes in two modes: para-positronium (p-Ps), where both particles have anti-parallel spin values, with a lifetime value around 125 ps; and ortho-positronium, with parallel spin particles, whose lifetime value ranges from 142 ns in a vacuum to a few nanoseconds in condensed matter [33–38]. The lifetime of o-Ps in condensed matter has been shown to be directly related to the size of the open-volume region. Further information on the relation between o-Ps lifetime and cavity size are detailed in the relevant methods section below.

In this present study PLA-PHBV blends with varying composition have been studied to characterize the physical structure and any relationship to the observed properties. Although similar studies have been performed on the blend systems described above, in this study the PALS methodology has been employed to determine the variation in size and relative concentration of free volume in the blends. There are no other reports in the literature of a similar study on this blend system, and it is hoped that the information obtained from PALS will provide further insight into the physical characteristics.

Materials and methods

Materials

The PLA (Ingeo™ Biopolymer 2003D) used in this study was obtained from NatureWorks LLC (USA). It is a transparent, high molar mass, biopolymer with a density of 1.24 g cm^{-3}, glass transition temperature of ~55 °C, and a melt temperature of ~150 °C. PHBV was purchased from Goodfellow (UK). It has a 12% hydroxy valerate (HV) content, a density of 1.24 g cm^{-3}, and a melt temperature of 156 °C.

Sample preparation

The samples were prepared via melt-mixing using a Brabender Plastograph. Prior to use, both polymers were placed in an oven, and dried overnight at 50 °C. The PLA/PHBV blend composition was varied from 10/90 to 90/10 *w/w* in 10 wt.% increments, and prepared by mixing at 180 °C for 10 min at a speed of 50 rpm. The samples were then compression moulded at 180 °C to the required thickness using a hydraulic press operating at a force of 1 ton.

Characterisation

The blend morphology was investigated using a field emission scanning electron microscope (FESEM), FEI Quanta 200, at an accelerating voltage of 15–20 kV. The samples were fractured in liquid nitrogen, and the fractured surfaces were sputter coated with gold for 90 s to eliminate sample charging.

The glass transition temperatures (T_g) were determined in a TA Instruments RSA G2 dynamic mechanical analyser (DMA) on samples with dimensions 10 mm × 50 mm × 2 mm. The experiments were performed in the bending mode with a frequency of 1 Hz. The samples were characterised over the temperature range − 25 to 100 °C at a heating rate of 3 °C min^{-1} under nitrogen atmosphere.

Tensile measurements were performed using dumbbell-shaped bars with a gauge length of 16 mm, a width of approximately 3.25 mm, from a thickness of 1 mm. The tests were carried out at room temperature using a Lloyd LF Plus 1 kN universal testing machine. Ten specimens of each composition were measured and analysed, and the average and standard deviation values are reported.

X-ray diffraction (XRD) spectra were recorded using a Panalytical X-ray diffractometer. These spectra were used to determine the degree of crystallinity (X_c) for each

of the prepared samples. Measurements were performed over a 2θ range of 10 to 60°. The crystallinity was determined with Eq. 1,

$$X_c(\%) = \left[\frac{A_C}{A_C + A_A}\right] \times 100 \quad (1)$$

where A_A is the area under the amorphous halo and A_C the remaining area under the crystalline regions.

The thermal conductivity (κ) was characterised using a Hot Disk TPS 2500S thermal constants analyser. Measurements were carried using two, nominally identical, samples, thickness 3 mm, sandwiched around the sensor probe for approximately 2 to 3 min. The method included one-dimensional heat flow only.

Positron annihilation lifetime spectroscopy (PALS) measurements were performed using conventional 'fast-fast' coincidence spectrometers from Ortec [39]. The Instrument Resolution Function (IRF) was determined to be approximately 180 ps using a well-annealed polycrystalline aluminium reference sample. Two nominally identical samples (thickness 1 mm) were placed either side of the positron source: ^{22}Na encapsulated between two sheets of 7.5 μm Kapton® foil (Dupont, USA). The obtained PALS spectra typically contained greater than five million coincidence counts, and were collected in a single 24 h period at room temperature (approximately 23 °C). Analyses were performed using the computer software package PALSfit and with appropriate source correction terms [40–43]. Satisfactory fits were obtained using four, unconstrained, positron component terms.

For a polymer system, positron lifetime values between 100 and 600 ps (τ_1 and τ_2) are typically attributed to para-positronium and/or positron annihilation, whereas lifetimes longer than 1 ns are associated with ortho-postironium (o-Ps) formation and, consequently, free volume [35–38]. These o-Ps lifetime values can be related to the size of the annihilation site by an empirical model (Eq. 2) that assumes a spherical cavity with radius (R) [33, 44–46].

$$\tau = \frac{1}{2}\left[1 - \frac{R}{R_0} + \frac{1}{2\pi}\sin\left(2\pi\frac{R}{R_0}\right)\right]^{-1} \quad (2)$$

where $R_0 = R + \Delta R$, and ΔR is empirically determined to be 1.656 Å. The average size of the free volume (V_F) can determined with Eq. 3,

$$V_F = \frac{4}{3}\pi R^3 \quad (3)$$

and the fractional free volume (F_V) with Eq. 4,

$$F_V = CV_F I \quad (4)$$

where I is the intensity value of the lifetime component obtained from PALS, and C a scaling factor that can be obtained from PVT experiments [33]. In the absence of such measurements the relative fractional free volume, $FFV = V_F I$, is reported.

Results and discussion

Blend morphology

Scanning electron microscopy (SEM) was used to investigate the morphology of the blends under study in order to provide further insight into the other determined properties.

A clear sea-island morphology is visible for each of the blends shown in Fig. 1, although there are indications of the formation of a co-continuous morphology in images (d) and (e) in Fig. 1. There is an increase in the size of the dispersed PHBV spheres as the PHBV content is increased from 10 wt.% to 50 wt.% in the blends, and one could assume that the sphere in Fig. 1(f) is PLA. At higher magnifications, cavities are clearly visible around the spheres, especially in Fig. 1(b) and 1(c), although bridges were observed in the cavities (image not shown). It appears as if there is fairly intimate contact between the two polymers, despite being clearly immiscible.

In all the images it is clear that there is fairly intimate contact between the continuous and dispersed polymers, but the spheres are fairly intact after liquid nitrogen fracturing, which confirms that the interfacial adhesion was insufficient to keep the spheres attached to the continuous matrix. Sufficiently strong interfacial adhesion would have given rise to fracturing of the spheres.

It should be noted that no clear trend was observed in the interfacial separation between the two polymers with increasing PHBV content. The separation varied between approximately 68 nm and 270 nm throughout the sequence. Further, due to the weak interfacial adhesion it was not possible to definitively identify voids or cavities that were not the result of fracturing. Nevertheless, the observed cavities had an approximate mean diameter between 100 nm and 367 nm.

Miscibility and glass transition

Miscibility in a polymer blend is often concluded upon the basis of the glass transition temperature (T_g), where a single T_g value indicates miscibility. In this study measurements were performed using DMA to obtain the glass transition temperatures (Fig. 2).

Measurements conducted using pure polymer samples gave T_g values of approximately 67 °C and 10 °C for PLA and PHBV, respectively. For the sequence of blends under study two T_g values were observed, consistent with earlier reports [16, 20–32]. The lower T_g value remained invariant

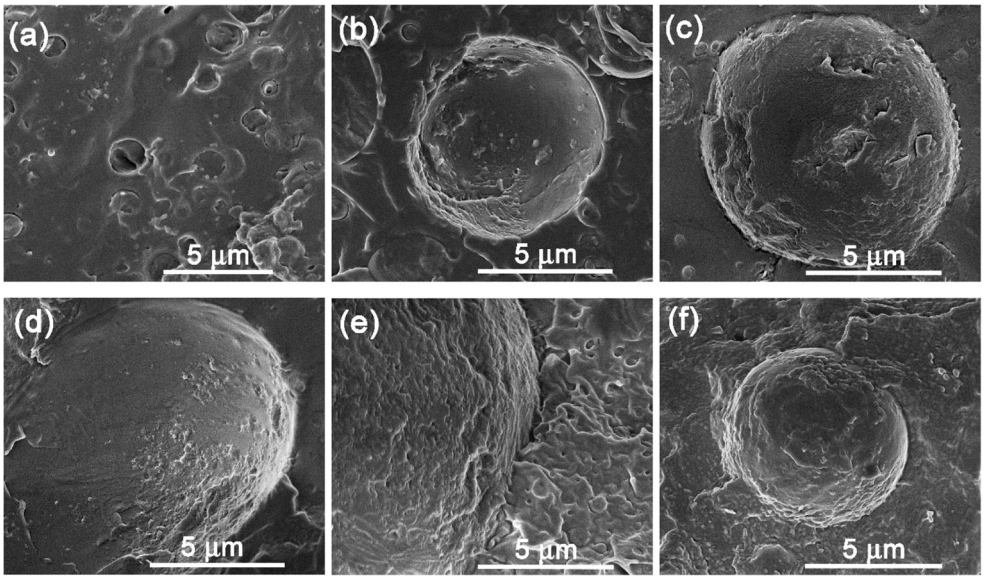

Fig. 1 SEM images of PLA/PHBV blends: **a** 90/10 *w/w* (25,000×), (**b**) 80/20 *w/w* (20,000×), (**c**) 70/30 *w/w* (25,000×), (**d**) 60/40 *w/w* (25,000×), (**e**) 50/50 *w/w* (25,000×), and (**f**) 40/60 *w/w* (25,000×)

at approximately 10 °C. In contrast, the higher T_g value decreased with increasing PHBV content, from 63 °C (90/10 *w/w* PLA/PHBV) to 55 °C (10/90 *w/w* PLA/PHBV). Similar behaviour has been reported by other authors [16, 20, 23–29]. The results indicate partial miscibility between the two polymers.

An interesting observation in Fig. 2 is that the neat PLA and the 10/90 *w/w* PLA/PHBV deviate from the almost perfect linearity of the decrease in T_gs observed for the other blends. It seems that at low PHBV contents, a greater percentage of the PHBV mixed with the PLA. The percentage miscibility of PHBV in PLA then remained fairly constant with increasing PHBV content, but at the highest PHBV content a smaller than expected percentage of PHBV mixed with the PLA.

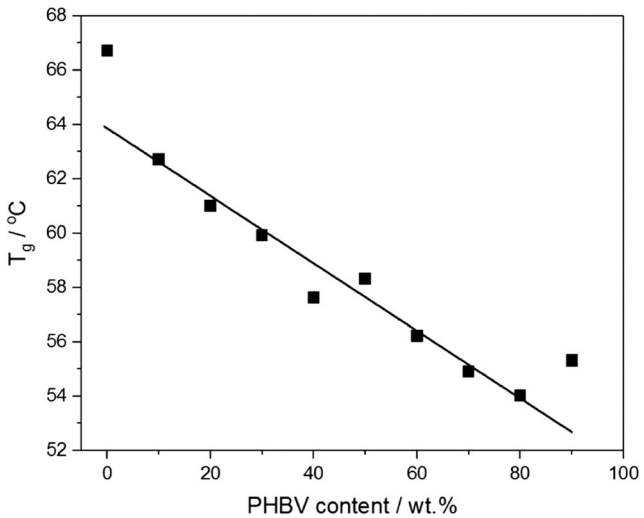

Fig. 2 Glass transition temperature (T_g) of PLA as a function of PHBV content for PLA/PHBV blends

Mechanical properties

Tensile measurements were performed for pure polymer samples and the PLA/PHBV blends. The obtained Young's modulus and tensile strength values are reported as a function of PHBV content in Fig. 3. It is immediately clear that PLA and PHBV exhibit similar tensile strength values (19.5 MPa and 20.4 MPa, respectively), as shown on Fig. 3(a); however, in the case of PLA the standard deviation in the measurement was considerable at approximately 11.0 MPa. Incorporation of 10 wt.% PHBV resulted in a significant increase in the strength (43.0 MPa), and suggests that the obtained values for pure PLA may be erroneous. On the other hand, this significant increase may have been the result of the higher percentage of (crystalline) PHBV that was miscible with the PLA, as was observed and discussed in the "Miscibility and glass transition" section. After this initial increase in tensile strength, a fairly significant decrease in tensile strength was observed as the PHBV content increased from 10 wt.% to 30 wt.%. This was probably the result of the weak interfacial forces between the constituent polymers, as discussed in the "Blend morphology" section. However, with a further increase in PHBV content, the tensile strength only slightly decreased and eventually levelled off around 20 MPa. This could be related to the absence of a typical co-continuous morphology in these blends, as can be seen from the images in Fig. 1.

The Young's modulus values show a trend similar to that of the trend observed for the tensile strength values (Fig. 3(b)). In this case, however, there is an almost linear decrease in Young's modulus from ~2 GPa for the 90/10 PLA/PHBV sample to 1.2 GPa for the 10/90 *w/w* PLA/PHBV sample. However, the deviation observed for the two neat polymers, where neat PLA has a significantly lower Young's modulus

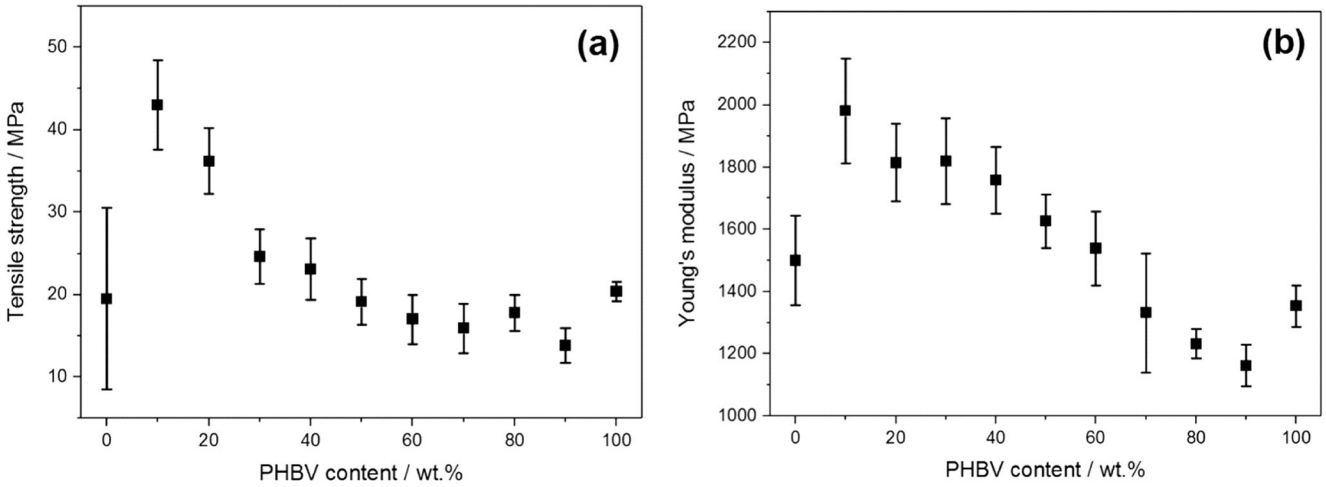

Fig. 3 Mechanical properties as a function of PHBV content for PLA/PHBV blends. Shown are (**a**) tensile strength and (**b**) Young's modulus

than the 90/10 *w/w* PLA/PHBV sample, and neat PHBV has a higher Young's modulus than the 10/90 *w/w* PLA/PHBV sample, is difficult to explain, but must be related to the atypical change in morphology as one goes from blends with high PLA contents to blends with low PLA contents. These results are consistent with similar observed trends reported in literature [16, 20–22].

X-ray diffraction

X-ray diffraction measurements were performed for the sequence of blended samples as well as for the pure polymers. The spectrum obtained for neat PLA (Fig. 4(a)) exhibited a broad halo which confirms the highly amorphous nature of the PLA. In contrast, neat PHBV exhibited two prominent peaks at approximately $2\theta = 13.5°$ and 16.9° (Fig. 4(a)), as well as a number of minor peaks (not shown). The prominent peaks were observed across for all the blended samples under study. The degree of crystallinity (X_c) was calculated using Eq. 1, and the results are illustrated in Fig. 4(b). The degrees of crystallinity calculated directly from the peak areas, without taking into account the PHBV contents in the respective samples, are shown as blue squares in the figure, while the degrees of crystallinity normalised with respect to the PHBV contents in the blends are shown as black circles.

Without normalisation the degrees of crystallinity generally increase with increasing PHBV content. PLA was found to be completely amorphous, even after controlled heating and cooling. Assuming the PLA does not crystallize when blended with PHBV, the crystalline peaks in the XRD spectra of the blends could only be related to the PHBV crystals. However, a very different picture emerges when one looks at the normalised X_c values in Fig. 4(b). One would expect some calculation inaccuracies at low PHBV contents because of the small crystalline peak sizes, and the fluctuation observed between 10 and 40 wt.% PHBV probably does not have any real significance. It is, however, interesting that the crystallinity seems to be high at low PHBV contents, then decreases fairly significantly between 50 and 80 wt.% PHBV, and then stabilizes at a value of about 70% between 80 and 100 wt.% PHBV. This could be the result of some PLA crystallization nucleated by the presence of PHBV crystals, as well as the absence of an obvious co-continuous morphology when changing the PLA:PHBV ratios from 90:10 to 10:90. It is also possible that crystallinity is being enhanced by the dispersed PHBV where it forms numerous, small, and highly crystalline regions or spheres [10, 25], or that the continuous PLA phase enhances the crystallization of PHBV. Increasing the PHBV content results in an increase in size of the PHBV phase, which seems to decrease the crystallinity to the level of that of neat PHBV. The very small PLA spheres in this concentration region obviously did not have any observable influence on the PHBV crystallization in this region.

Thermal conductivity

The results from thermal conductivity (κ) measurements are shown in Fig. 5. The obtained values for neat PLA and neat PHBV were nominally similar at approximately 0.21 W m^{-1} K^{-1} and 0.23 W m^{-1} K^{-1}, respectively. For the sequence of blended samples, the thermal conductivity was observed to increase with increasing PHBV content, and were in close agreement with the weighted average values. The results are in agreement with the expectation that amorphous materials typically exhibit lower thermal conductivity than crystalline materials [47].

Positron annihilation lifetime spectroscopy (PALS)

The obtained PALS spectra were analysed using an unconstrained four-term fit with the fitting software PALSfit and required two ortho-positronium (o-Ps) component terms (τ_3

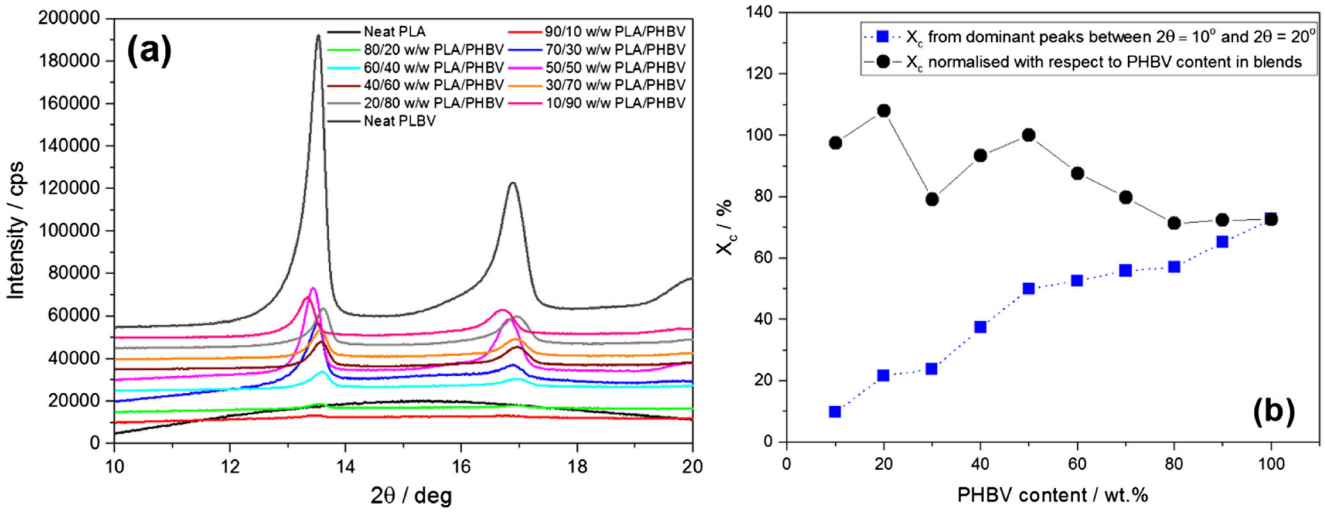

Fig. 4 **a** XRD spectra of all the investigated samples; (**b**) Degree of crystallinity (X_c) as a function of PHBV content, as calculated and normalized with respect to PHBV content in blends

and τ_4 with intensities I_3 and I_4, respectively) throughout the sample range under study. Figure 6 details the obtained o-Ps lifetime (a) and intensity (b) values.

From the obtained positron lifetime data, it is immediately clear that the o-Ps component terms exhibit some variation with blend composition. The first o-Ps component (circles) exhibited similar lifetime values, Fig. 6(a), for the sequence of blends and had a mean value of approximately 1.20 ns. In contrast, the intensity values, Fig. 6(b), exhibited an increase with increasing PHBV content. The deviation of this term from the predicted weighted average values suggest that the origin of this term is being influenced by the interaction between the two polymers.

The second o-Ps component (squares) terms exhibited a more marked variation and increased with PHBV content. The lifetime values exhibited a weak negative deviation relative to the weighted average values, whilst the intensity values increased almost linearly. Furthermore, the lifetime and intensity values were greater for PHBV than for PLA. The o-Ps lifetime values (τ_4) can be related to the mean size of the annihilation site using the semi-empirical expression in Eq. 2 and assuming a spherical cavity (Eq. 3). The calculated values are detailed in Table 1. In accordance with the lifetime values, the mean free volume of the annihilation site increases with PHBV content and is larger for neat PHBV than for neat PLA.

The variation of relative fractional free volume (FFV) is shown in Fig. 7. The behaviour is similar, but less marked, to that observed for the second o-Ps lifetime component (τ_4). The calculated values are close to those predicted by weighted average and exhibit a linear increase with increasing PHBV content. It is further interesting to note that the exhibited behaviour of FFV with PHBV content mirrors the observed trends for crystallinity and thermal conductivity, and suggests some complex relationship between the three parameters [48].

The results detailed above for the second o-Ps component support the conclusion that the mean volume of voids in the series of blends under study are influenced by more than just the relative weight fraction of the constituent polymers. Furthermore, the influence results in a suppression in cavity size which reaches a maximum effect around 30 wt.% PHBV.

The origin of these o-Ps component terms in polymer systems have been described in literature as either due to o-Ps formation in amorphous or crystalline regions, at intermolecular sites or voids It can be immediately discounted that either of the o-Ps components arise solely due to formation in the amorphous regions. Analyses from XRD indicated a clear increase in crystallinity with increasing PHBV content, and, therefore, one would expect a decrease in the relative intensity of either component term with PHBV content. Furthermore,

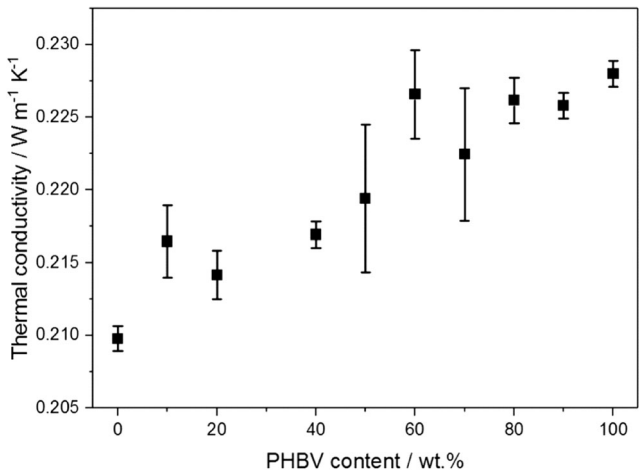

Fig. 5 Thermal conductivity as a function of PHBV content for PLA/PHBV blends

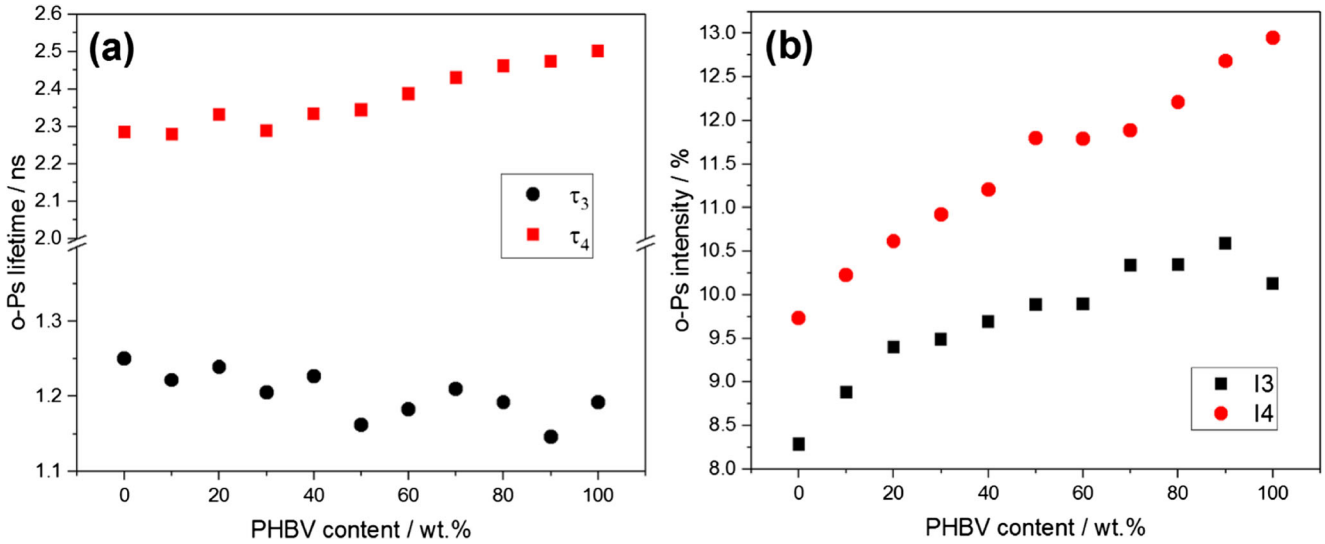

Fig. 6 Obtained ortho-Positronium (o-Ps) component terms as a function of PHBV content in PLA/PHBV. Shown are (**a**) lifetime, and (**b**) intensity

the highly amorphous nature of pure PLA should result in a markedly greater intensity component than the semi-crystalline pure PHBV. It is, therefore, likely that o-Ps formation is occurring at both the amorphous and crystalline regions, and that the semi-crystalline PHBV exhibits larger free volume sites with greater concentration than the amorphous PLA.

Finally, it should be noted that either o-Ps term does not solely originate at any interfacial region between the two polymers due to the presence of both terms across the sequence of samples studied. Although the SEM images provided clear evidence of interfacial cavities in the order of approximately 70 nm and voids around 100 to 400 nm in diameter, the greater resolution of PALS observed sub-nanometre voids and may suggest that o-Ps formation is occurring between polymer chains in the large open volume regions [35].

Table 1 Mean free volume of voids in PLA/PHBV blends as a function of PHBV content

PHBV content / wt.%	Mean free volume / Å^3
0	124
10	124
20	129
30	125
40	129
50	130
60	135
70	139
80	142
90	143
100	146

Conclusions

Polymer blends of PLA and PHBV were prepared by melt mixing. The morphology and physical properties of the blends were investigated along with those of the neat polymers. SEM studies provided evidence of interfacial cavities and weak interfacial interaction between the two polymers. No definitive co-continuous morphology was observed in the sequence of blends under study. Characterisation using the PALS method indicated the presence of open-volume cavities with sub-nanometre diameters; far smaller than observed from the SEM images. Furthermore, the mean size and relative concentration of these cavities increased with increasing PHBV content. A weak negative deviation, from the weighted average values, in the mean size for low PHBV content was observed, and possibly indicates some degree of partial miscibility. The

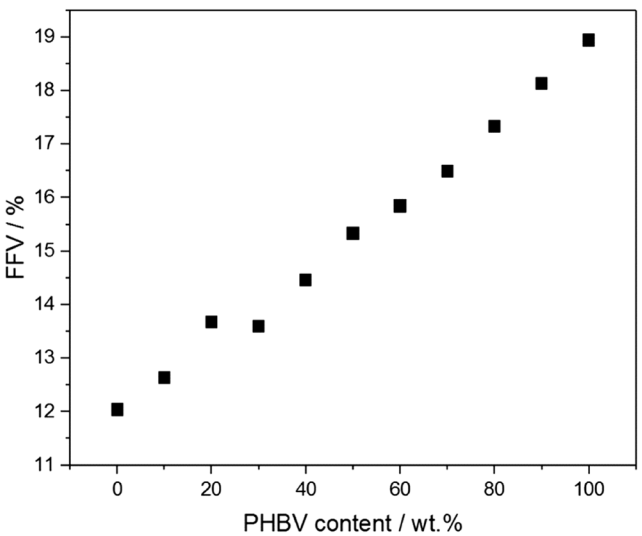

Fig. 7 Obtained relative fractional free volume (FFV) from PALS measurements as a function of PHBV content for PLA/PHBV blends

glass transition temperature of PLA in the blends decreased with increasing PHBV content, and offers support to the partial miscibility in the blends. The normalised degree of crystallinity for the blends was high when PHBV was the minority phase, but decreased as PHBV became the continuous phase. The thermal conductivity of the samples varied with composition. The observed increase with increasing PHBV content is likely related to the increasing crystallinity exhibited in the sequence of samples studied.

The mechanical properties from tensile testing showed a decrease in both tensile strength and Young's modulus with increasing PHBV for the sequence of blends. In addition, both parameters exhibited maximum values for 10 wt.% PHBV. For samples between 50/50 and 10/90 PLA/PHBV the tensile strength and Young's modulus were comparable to or lower than those for either of the neat polymers.

Acknowledgements This publication was made possible by PDRA grant PDRA2-1118-14127 from the Qatar National Research Fund (a member of Qatar Foundation). The findings achieved herein are solely the responsibility of the authors.

References

1. Siracusa V, Rocculi P, Romani S, Dalla Rosa M (2008) Biodegradable polymers for food packaging: a review. Trends Food Sci Technol 19:634–643
2. Rivera-Gómez C, Galán-Marín C (2017) Biodegradable fiber-reinforced polymer composites for construction applications. In: natural Fiber-reinforced biodegradable and Bioresorbable polymer composites. Woodhead Publishing, Elsevier, Amsterdam
3. Facchetti A (2011) π-Conjugated polymers for organic electronics and photovoltaic cell applications. Chem Mater 23:733–758
4. Patil A, Patel A, Purohit R (2017) An overview of polymeric materials for automotive applications. Mater Today: Proc 4:3807–3815
5. Derraik JGB (2002) The pollution of the marine environment by plastic debris: a review. Mar Pollut Bull 44:842–852
6. McKeen LW (2014) Plastics used in medical devices A2 - Modjarrad, Kayvon. In: Ebnesajjad S (ed) Handbook of polymer applications in medicine and medical devices. Oxford, William Andrew Publishing
7. Garlotta D (2001) A literature review of poly(lactic acid). J Polym Environ 9:63–84
8. Auras R, Harte B, Selke S (2004) An overview of polylactides as packaging materials. Macromol Biosci 4:835–864
9. Castro-Aguirre E, Iñiguez-Franco F, Samsudin H, Fang X, Auras R (2016) Poly(lactic acid) - mass production, processing, industrial applications, and end of life. Adv Drug Deliv Rev 107:333–366
10. Zhang M, Thomas NL (2011) Blending polylactic acid with polyhydroxybutyrate: the effect on thermal, mechanical, and biodegradation properties. Adv Polym Technol 30:67–79
11. Mofokeng J, Luyt AS (2015) Morphology and thermal degradation studies of melt-mixed poly(lactic acid) (PLA)/poly(ε-caprolactone) (PCL) biodegradable polymer blend nanocomposites with TiO_2 as filler. Polym Test 45:93–100
12. Farah S, Anderson DG, Langer R (2016) Physical and mechanical properties of PLA, and their functions in widespread applications - a comprehensive review. Adv Drug Deliv Rev 107:367–392
13. Verhoogt H, Ramsay BA, Favis BD (1994) Polymer blends containing poly(3-hydroxyalkanoate)s. Polymer 35:5155–5169
14. Liu Q, Shyr T-W, Tung C-H, Deng B, Zhu M (2011) Block copolymers containing poly(3-hydroxybutyrate-co-3-hydroxyvalerate) and poly(ε-caprolactone) units: synthesis, characterization and thermal degradation. Fiber Polym 12:848–856
15. El-Hadi A, Schnabel R, Straube E, Müller G, Henning S (2002) Correlation between degree of crystallinity, morphology, glass temperature, mechanical properties and biodegradation of poly(3-hydroxyalkanoate) PHAs and their blends. Polym Test 21:665–674
16. Nanda MR, Misra M, Mohanty AK (2011) The effects of process engineering on the performance of PLA and PHBV blends. Macromol Mater Eng 296:719–728
17. Modi S, Koelling K, Vodovotz Y (2011) Assessment of PHB with varying hydroxyvalerate content for potential packaging applications. Eur Polym J 47:179–186
18. Koning C, Van Duin M, Pagnoulle C, Jerome R (1998) Strategies for compatibilization of polymer blends. Prog Polym Sci 23:707–757
19. Zhang K, Mohanty AK, Misra M (2012) Fully biodegradable and biorenewable ternary blends from polylactide, poly(3-hydroxybutyrate-co-hydroxyvalerate) and poly(butylene succinate) with balanced properties. ACS Appl Mater Interf 4:3091–3101
20. Zhao H, Cui Z, Sun X, Turng L-S, Peng X (2013) Morphology and properties of injection molded solid and microcellular polylactic acid/polyhydroxybutyrate-valerate (PLA/PHBV) blends. Ind Eng Chem Res 52:2569–2581
21. Ma P, Spoelstra AB, Schmit P, Lemstra PJ (2013) Toughening of poly(lactic acid) by poly(β-hydroxybutyrate-co-β-hydroxyvalerate) with high β-hydroxyvalerate content. Eur Polym J 49:1523–1531
22. Liu Q, Wu C, Zhang H, Deng B (2015) Blends of polylactide and poly(3-hydroxybutyrate-co-3-hydroxyvalerate) with low content of hydroxyvalerate unit: morphology, structure, and property. J Appl Polym Sci 132:42689
23. Zembouai I, Bruzaud S, Kaci M, Benhamida A, Corre Y-M, Grohens Y, Lopez-Cuesta J-M (2014) Synergistic effect of compatibilizer and Cloisite 30B on the functional properties of poly(3-hydroxybutyrate-co-3-hydroxyvalerate)/polylactide blends. Polym Eng Sci 54:2239–2251
24. Zembouai I, Bruzaud S, Kaci M, Benhamida A, Corre Y-M, Grohens Y, Taguet A, Lopez-Cuesta J-M (2014) Poly(3-hydroxybutyrate-co-3-hydroxyvalerate)/polylactide blends: thermal stability, flammability and thermo-mechanical behavior. J Polym Environ 22:131–139
25. Zembouai I, Kaci M, Bruzaud S, Benhamida A, Corre Y-M, Grohens A (2013) A study of morphological, thermal, rheological and barrier properties of poly(3-hydroxybutyrate-co-3-hydroxyvalerate)/polylactide blends prepared by melt mixing. Polym Test 32:842–851
26. González-Ausejo J, Gámez-Pérez J, Balart R, Lagarón JM, Cabedo L (2017) Effect of the addition of sepiolite on the morphology and properties of melt compounded PHBV/PLA blends. Polym Compos. https://doi.org/10.1002/pc.24538
27. Richards E, Rizvi R, Chow A, Naguib H (2008) Biodegradable composite foams of PLA and PHBV using subcritical CO_2. J Polym Environ 16:258–266
28. Mofokeng JP, Luyt AS (2015) Dynamic mechanical properties of PLA/PHBV, PLA/PCL, PHBV/PCL blends and their nanocomposites with TiO_2 as nanofiller. Thermochim Acta 613:41–53
29. Gerard T, Budtova T (2012) Morphology and molten-state rheology of polylactide and polyhydroxyalkanoate blends. Eur Polym J 48:1110–1117
30. Ferreira B, Zavaglia C, Duek E (2002) Films of PLLA/PHBV: thermal, morphological, and mechanical characterization. J Appl Polym Sci 86:2898–2906

31. Modi S, Koelling K, Vodovotz Y (2012) Miscibility of poly(3-hydroxybutyrate-co-3-hydroxyvalerate) with high molecular weight poly(lactic acid) blends determined by thermal analysis. J Appl Polym Sci 124:3074–3081
32. González-Ausejo J, Sánchez-Safont E, Lagarón JM, Balart R, Cabedo L, Gámez-Pérez J (2017) Compatibilization of poly(3-hydroxybutyrate-co-3-hydroxyvalerate)–poly(lactic acid) blends with diisocyanates. J Appl Polym Sci **134**(20):N/a–n/a
33. Jean Y, Mallon PE, Schrader D (2003) Principles and applications of positron and Positronium chemistry. World Scientific, London
34. Jean YC (1990) Positron annihilation spectroscopy for chemical analysis: a novel probe for microstructural analysis of polymers. Microchem J 42:72–102
35. Dlubek G, Kilburn D, Bondarenko V, Pionteck J, Krause-Rehberg R, Ashraf Alam M (2004) Positron annihilation: a unique method for studying polymers. Macromol Symp 210:11–20
36. Dlubek G, Stejny J, Lüpke T, Bamford D, Petters K, Hübner C, Alam MA, Hill MJ (2002) Free-volume variation in polyethylenes of different crystallinities: positron lifetime, density, and X-ray studies. J Polym Sci B Polym Phys 40:65–81
37. Machado JC, Silva GG, de Oliveira FC, Lavall RL, Rieumont J, Licinio P, Windmöller D (2007) Free-volume and crystallinity in low molecular weight poly (ethylene oxide). J Polym Sci B Polym Phys 45:2400–2409
38. Madani MM, MacQueen RC, Granata RD (1996) Positron annihilation lifetime study of PTFE/silica composites. J Polym Sci B Polym Phys 34:2767–2770
39. Krause-Rehberg R, Leipner HS (1999) Positron annihilation in semiconductors: defect studies. Springer Verlag Berlin Heidelberg
40. Olsen JV, Kirkegaard P, Pedersen NJ, Eldrup M (2007) PALSfit: a new program for the evaluation of positron lifetime spectra. Phys Status Solidi (c) 4:4004–4006
41. Staab T, Somieski B, Krause-Rehberg R (1996) The data treatment influence on the spectra decomposition in positron lifetime spectroscopy part 2: the effect of source corrections. Nucl Instr Meth Phys Res A 381:141–151
42. McGuire S, Keeble D (2006) Positron lifetimes of polycrystalline metals: a positron source correction study. J Appl Phys 100:103504
43. Kanda GS, Keeble DJ (2016) Positron annihilation lifetime spectroscopy source correction determination: a simulation study. Nucl Instr Meth Phys Res A 808:54–59
44. Tao SJ (1972) Positronium annihilation in molecular substances. J Chem Phys 56:5499–5510
45. Eldrup M, Lightbody D, Sherwood JN (1981) The temperature dependence of positron lifetimes in solid pivalic acid. Chem Phys 63:51–58
46. Dlubek G, Taesler C, Pompe G, Pionteck J, Petters K, Redmann F, Krause-Rehberg R (2002) Interdiffusion in a particle matrix system of two miscible polymers: an investigation by positron annihilation lifetime spectroscopy and differential scanning calorimetry. J Appl Polym Sci 84:654–664
47. Kline DE (1961) Thermal conductivity studies of polymers. J Polym Sci 50:441–450
48. Dlubek G, Saarinen K, Fretwell HM (1998) The temperature dependence of the local free volume in polyethylene and polytetrafluoroethylene: a positron lifetime study. J Polym Sci B Polym Phys 36:1513–1528